

Journal of Advanced Research in Computing and Applications





Optimization of SnO₂ Concentration in PVDF-Based Piezoelectric Nanocomposites for Enhanced Energy Harvesting at Low Frequencies

Muhammad Amir Zarif Azrai¹, Abdul Malek Abdul Wahab^{1,*}, Habibah Zulkefle², Muhamad Sukri Hadi¹

- ¹ School of Mechanical Engineering, Universiti Teknologi MARA (UiTM), 40450 Shah Alam, Selangor, Malaysia
- School of Electrical Engineering, Universiti Teknologi MARA (UiTM), 40450 Shah Alam, Selangor, Malaysia

ARTICLE INFO

Article history:

Received 17 February 2025 Received in revised form 30 May 2025 Accepted 6 August 2025 Available online 3 September 2025

Keywords:

Piezoelectric; Cantilever Beam; vibration energy harvesting; Polyvinyledene Flouride (PVDF); tin oxide

ABSTRACT

This study investigates the influence of varying SnO_2 concentrations in PVDF-based piezoelectric nanocomposites on electrical output under different frequency conditions. Three different weight percentages (3 wt%, 5 wt%, and 7 wt%) were tested to determine the optimal concentration for energy harvesting applications. The results revealed that a 5 wt% SnO_2 concentration produced the highest electrical output, achieving a peak voltage of 0.6 V and maximum power at approximately 6 Hz, which aligns with the system's natural resonance frequency. Higher SnO_2 concentrations (7 wt%) resulted in reduced performance due to increased stiffness, while the lower concentration (3 wt%) showed consistent output but lower peak values, demonstrating its suitability for stable, low-frequency applications. These findings emphasize the importance of material composition and frequency optimization for enhancing energy conversion efficiency in piezoelectric systems. The study contributes valuable insights into the design of piezoelectric energy harvesting devices, particularly for applications in low-frequency environments.

1. Introduction

The global energy demand continues to rise, necessitating the exploration of innovative methods for sustainable energy harvesting, particularly from ambient sources such as low-frequency vibrations. Piezoelectric materials have emerged as effective candidates for this purpose, given their intrinsic capability to convert mechanical energy into electrical energy. For instance, a microfabricated piezoelectric cantilever demonstrated a power output of 0.491 μ W at a resonance frequency of 163 Hz under specific vibration intensities of 10 m/s². Similarly, a MEMS-based arrayed harvester produced 6.8 μ W of power at frequencies ranging between 67–70 Hz, showcasing the efficacy of these systems in such applications [26]. Recent research has focused on harnessing low-

E-mail address: abdmalek@uitm.edu.my

https://doi.org/10.37934/arca.39.1.181195

^{*} Corresponding author.

frequency ambient vibrations using cantilever systems integrated with piezoelectric materials, highlighting their potential for developing self-powered systems [13].

Despite these advances, many devices still exhibit power limitations as excitation frequencies decrease, necessitating the development of more innovative designs like multi-impact harvesters, which have shown up to three times the power output of traditional setups. The need for optimization in energy conversion efficiency, particularly at lower frequencies, remains a critical area of focus [13].

Optimizing the properties of piezoelectric materials, particularly for low-frequency applications, is essential for enhancing energy conversion efficiency. Utilizing PVDF in an optimized cantilever configuration achieved an output power density of $112.8\,\mu\text{W}$ within a compact volume of $13.1\,\text{mm}^3$, aligning its performance with that of piezoceramic devices [21]. Studies have demonstrated that using Zinc Oxide (ZnO) on Aluminium substrates achieved peak power values of $4.02\,\text{mW}$ at $170\,\text{Hz}$, emphasizing the critical role of material integration. Multi-material approaches combining piezoelectric and non-piezoelectric elements have also proven effective in tuning material distribution within composite structures, resulting in improved efficiency [5]. More recently, a PVDF-based cantilever system optimized for resonance at $14.3\,\text{Hz}$ yielded a maximum power output of $104.38\,\text{mW}$, showcasing advancements in low-frequency energy harvesting [22]. However, challenges remain, especially in scaling these systems for practical use.

Optimizing the properties of piezoelectric materials, particularly for low-frequency applications, is essential for enhancing energy conversion efficiency. Utilizing PVDF in an optimized cantilever configuration achieved an output power density of 112.8 μ W within a compact volume of 13.1 mm³, aligning its performance with that of piezoceramic devices [21]. Studies have shown that using Zinc Oxide (ZnO) on Aluminium substrates achieved peak power values of 4.02 mW at 170 Hz, emphasizing the critical role of material integration. A PVDF-based cantilever system optimized for resonance at 14.3 Hz yielded a maximum power output of 104.38 mW, showcasing advancements in low-frequency energy harvesting [22]. Furthermore, multi-material approaches combining piezoelectric and non-piezoelectric elements have proven effective in tuning material distribution within composite structures, resulting in improved efficiency [5]. However, challenges remain, especially in scaling these systems for practical use.

Low-frequency vibrations, prevalent in various environments, offer a promising but underutilized energy source. However, despite advancements in piezoelectric systems, several challenges persist. Existing designs often exhibit suboptimal energy conversion efficiency under low-frequency conditions, and there is a lack of a comprehensive framework that integrates material selection. Therefore, this work focuses on investigating the significant of material properties in optimized energy harvesting of piezoelectric cantilever beams at low-frequency vibration. The piezoelectric cantilever beams were evaluated by applying different SnO₂ concentrations within PVDF-based piezoelectric nanocomposites. Different weight percentages were tested to determine the optimal concentration for energy harvesting applications.

2. Material and Method

2.1 Piezoelectric System

The piezoelectric material used in this work is PVDF/SnO₂ Flexible Piezoelectricc Nano-Generator (FPENG) film. Tin (IV) Oxide (SnO₂) was incorporated into the polyvinylidene fluoride (PVDF) matrix at varying weight percentages (3 wt%, 5 wt%, and 7 wt%) to investigate its effect on the properties of PVDF/SnO₂ FPENG films. The addition of SnO₂ nanoparticles is expected to enhance both structural and functional characteristics of the composite by influencing the crystallinity, phase formation, and

dispersion within the polymer matrix. Specifically, the SnO_2 nanoparticles promote the formation of the electroactive β -phase in PVDF, which is critical for maximizing piezoelectric output. The inclusion of SnO_2 improves the mechanical properties, such as flexibility and tensile strength, while also enhancing the surface hydrophobicity of the films, a feature that is crucial for energy harvesting applications. Studies have demonstrated that the incorporation of SnO_2 nanosheets significantly enhances the electroactive phase in PVDF and improves its piezoelectric performance [6]. Additionally, variations in nanoparticle content are known to optimize properties such as crystallinity and energy conversion efficiency, as observed in other piezoelectric composite studies [28,].

The SnO_2 content in this study was limited to 3 wt%, 5 wt%, and 7 wt% to avoid particle agglomeration, which becomes increasingly significant at higher filler loadings [15]. Excessive SnO_2 concentrations can lead to poor dispersion due to the intrinsic tendency of nanoparticles to aggregate, especially beyond 7 wt% [11]. This aggregation disrupts the uniformity of the composite and limits the effective interfacial interaction between SnO_2 and the PVDF matrix [10]. More importantly, agglomeration has been shown to inhibit the nucleation of the electroactive β -phase in PVDF, which directly affects the piezoelectric output [24]. Several studies have reported that beyond an optimal filler threshold, the β -phase content decreases due to these agglomeration effects, resulting in diminished dielectric and piezoelectric properties. Therefore, the selected weight percentages represent a practical and widely accepted range that promotes β -phase formation while minimizing the risk of microstructural defects that could compromise energy harvesting performance.

Therefore, in this study, SnO_2 powder is utilized as the filler for the PVDF solution to enhance the properties of the resulting composite. The effects of SnO_2 filler loading on the performance of the PVDF-based FPENG are systematically investigated. The study examines how varying SnO_2 concentrations influence the piezoelectric output and of the deposited PVDF/ SnO_2 FPENG films. Proper dispersion of SnO_2 enhances the formation of the electroactive β -phase, a critical crystalline structure for piezoelectric performance [6]. By analyzing these properties, this research aims to determine the optimal SnO_2 loading for improving energy harvesting efficiency, mechanical stability, and overall functionality [28].

The fabrication process involves the preparation of PVDF/SnO $_2$ FPENG films using a drop casting method followed by an annealing process at a temperature of 120°C. Initially, the PVDF polymer and Tin (IV) Oxide (SnO $_2$) were dissolved and uniformly mixed in an appropriate solvent to ensure homogeneous dispersion of the SnO $_2$ particles within the PVDF matrix. The resulting mixture was then cast onto a clean substrate to form a thin film. The films were subjected to the annealing process at 120°C to enhance the crystallinity and promote the formation of the electroactive β -phase in PVDF, which is crucial for improved piezoelectric performance. This annealing step also facilitated solvent evaporation, leading to mechanically stable and uniform films. The final PVDF/SnO $_2$ FPENG films were subsequently peeled off from the substrate and cut into desired dimensions for further characterization and application in energy harvesting devices.

Table 1 shows the wettability properties of PVDF/SnO₂ FPENG films at different SnO₂ loading percentages (wt%). The differences relate to the percentage of Tin (IV) Oxide (SnO₂) in Polyvinylidene Fluoride (PVDF). PVDF thin films with higher SnO₂ content have shown improved performance in several areas. The addition of SnO₂ can enhance the piezoelectric properties by increasing the β -phase content of PVDF, which improves energy harvesting efficiency [4]. Furthermore, as shown in Table 1, these thin films exhibited hydrophobic characteristics, with water contact angles above 90°, which are associated with water-repellent behavior, enhancing their durability in harsh environments [1]. Such hydrophobicity prevents water from contacting the substrate, leading to increased durability and suitability for long-term device applications.

Table 1Wettability Properties of PVDF/SnO₂ FPENG films

SnO ₂ Loading Percentage (wt%)	Dimension (cm ²)	Left Angle	Right Angle
3	2	96.50°	94.70°
5	2	97.60°	96.50°
7	2	94.80°	97.60°

2.2 Experimental Setup

The cantilever beam system was designed to convert low-frequency ambient vibrations into electrical energy using the piezoelectric effect. The experimental setup in Figure 1 illustrates the process for analyzing a cantilever system with a piezoelectric element. The piezoelectric material was affixed to a metal ruler, with one end clamped to the support structure and the other end loaded with a mass. The system was excited using a function generator connected to a shaker, producing vibrations across a frequency range of 0 Hz to 20 Hz in 1 Hz increments. Each frequency was tested for 4 minutes, with 2 minutes allotted for normalizing the polarization and 2 minutes for data collection via an oscilloscope. The setup was carefully calibrated to ensure that maximum beam deflection occurred at the point of piezoelectric attachment, maximizing energy conversion [24].

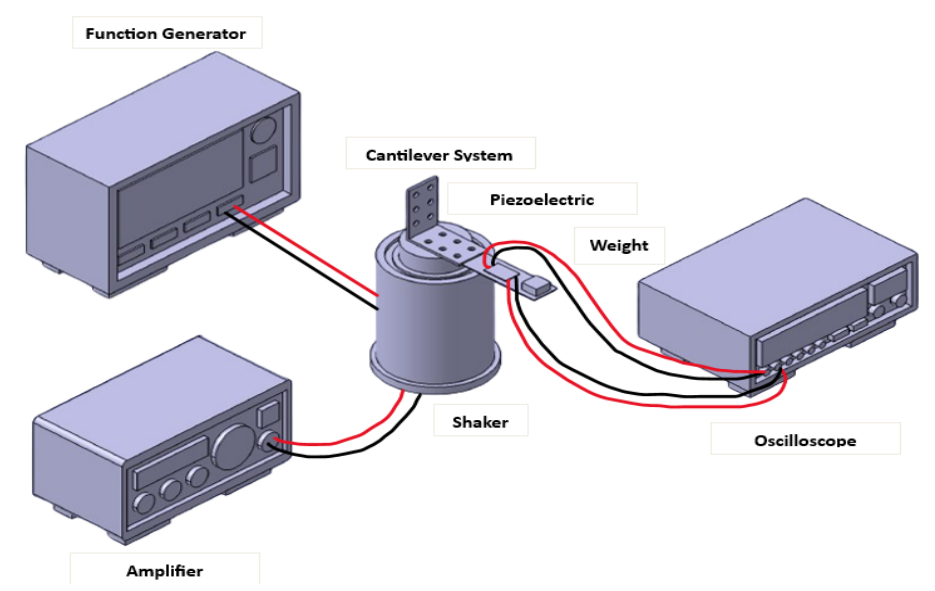


Fig. 1. Experimental Setup



Fig. 2. (a) Piezoelectric patch attached to the ruler; (b) Weight at the other end of the ruler

Table 2

Experimental	setun	specifications	and	nronerties
LADEIIIIICIII	SCLUP	3pecifications	anu	מו טעכו נוכט

Factors	Value
Frequency (Hz)	1 - 20
Weight percent (%), wt%	3, 5, 7

2.3 Design of Experiment

The experimental design aimed to evaluate the performance of the piezoelectric system by varying the weight percentages of Tin (IV) Oxide (SnO₂) in PVDF composites, with compositions of 3 wt%, 5 wt%, and 7 wt% [8]. Design Expert 13 software was used to plan, conduct, and analyze the experimental results, which included examining the effects of different vibration frequencies and SnO₂ weight percentages on the energy output [25]. The factors and response variables, such as voltage output and current, were input into the software, which generated an experimental design for optimizing performance. Graphical analysis was performed on the data collected from the experiments to assess the system's performance across different weight percentages of SnO₂ and frequency ranges. The analysis included voltage and current measurements under various conditions, helping to identify the best-performing specimen [1]. The analysis provided insights into the relationship between material composition, frequency, and energy output, with graphical representations confirming trends in system performance. A post-analysis procedure was conducted to validate the results and determine the optimal design for energy harvesting. The software suggested additional experiments based on the initial findings, which were conducted to verify the accuracy of the results [17]. This iterative process ensured that the final design offered the highest possible energy output for the given material composition and experimental setup. The experimental design is summarized in Table 3, which outlines the key parameters tested, including voltage output, current, and power generated under varying SnO₂ weight percentages and vibration frequencies. This comprehensive design facilitated a systematic investigation of the factors influencing energy harvesting performance, providing a clear framework for optimizing piezoelectric system design.

Table 3 summarizes data from experiments generated using Design Expert 13, with factors being the weight percentage of SnO_2 and frequency. The responses include the voltage produced (peak to peak), voltage drop, current produced, and power. The experiments vary the weight percentage and frequency to study their effects on the piezoelectric system's electrical output, with values recorded for each response. The power output increases with both voltage and current under different conditions of weight percentage and frequency, indicating the system's performance across these variables.

Table 3Table of data recommended by Design Expert 13

	40.0 0. 44.44 1.000							
Std Run	Factor 1	Factor 2	Response 1	Response 2	Response 3	Response 4		
	A: Weight Percent	B: Frequency	Voltage Produce (Peak to Peak)	Voltage Drop	Current Produced	Power		
	wt%	Hz	V	V	Α	W		
7	1	5	1	0.112	0.006032	0.006032	0.000675584	
12	2	5	10.5	0.175	0.00896	0.00896	0.001568	
8	3	5	20	0.1016	0.0064	0.0064	0.00065024	

Table 3 (continued)

		Factor 1	Factor 2	Response 1	Response 2	Response 3	Response 4
Std	Run	A: Weight Percent	B: Frequency	Voltage Produce (Peak to Peak)	Voltage Drop	Current Produced	Power
		wt%	Hz	V	V	Α	W
11	4	5	10.5	0.175	0.00896	0.00896	0.001568
4	5	7	20	0.088	0.0058	0.0058	0.0005104
5	6	3	10.5	0.1088	0.0052	0.0052	0.00056576
3	7	3	20	0.0762	0.004	0.004	0.0003048
9	8	5	10.5	0.175	0.00896	0.00896	0.001568
6	9	7	10.5	0.138	0.0067	0.0067	0.0009246
1	10	3	1	0.0922	0.00466	0.00466	0.000429652
2	11	7	1	0.1016	0.0057	0.0057	0.00057912
10	12	5	10.5	0.175	0.00896	0.00896	0.001568

To measure the current generated by the piezoelectric cantilever, a 1 Ω precision resistor was soldered in series with the output cable and connected across the terminals of the piezoelectric element. The oscilloscope probe was clipped across the resistor to monitor the voltage drop during beam vibration. This voltage drop was used to calculate the output current based on Ohm's law, using the relation

$$I = \frac{V}{R} \tag{1}$$

Where V is the measured voltage across the resistor and R is the known resistance (1 Ω). This setup allowed real-time current estimation during energy harvesting under varying vibration frequencies. The output power generated by the piezoelectric cantilever was calculated using the relation

$$P = IV (2)$$

Voltage was measured as peak-to-peak using the oscilloscope, while current was determined from the measured voltage drop across a 1 Ω resistor using Ohm's law. The peak-to-peak voltage and the corresponding calculated current were then used to estimate the instantaneous power output for each frequency condition.

3. Results and Discussion

3.1 Vibration Energy Production

Figure 3 shows how the voltage varies with frequency for three different weight percentages of SnO₂ in PVDF (3wt%, 5wt%, and 7wt%). The 5wt% sample demonstrates the highest peak, reaching over 0.6 V at approximately 6 Hz. This peak is likely due to resonance, where the system's natural frequency aligns with the applied mechanical vibration, leading to efficient energy transfer. The 7wt% sample follows with a peak voltage of around 0.45 V, while the 3wt% sample produces the lowest peak voltage of approximately 0.35 V. Beyond 7 Hz, voltage output decreases significantly for all samples and stabilizes as the frequency approaches 20 Hz. The results suggest that 5wt% is the optimal SnO₂ concentration because it balances flexibility and charge transfer. In contrast, 7wt%

likely results in material stiffness, reducing the ability to generate high voltage despite the higher SnO_2 content. These findings align with the overall behavior of piezoelectric and triboelectric materials, where resonance frequencies maximize energy output [27].

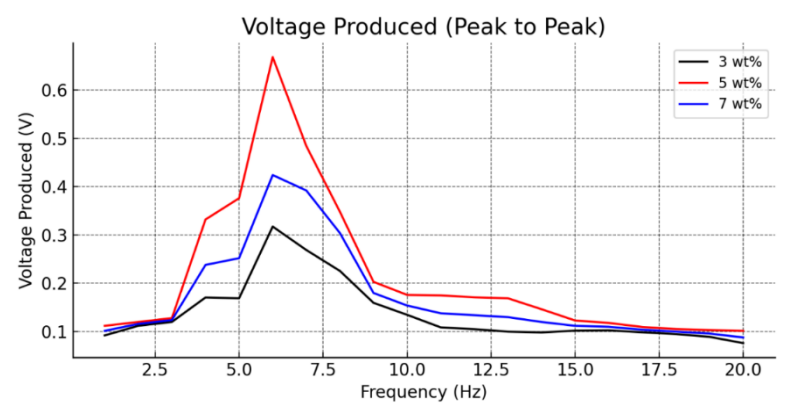


Fig. 3. Effect of different weight percent and frequency on Voltage Produced (Peak to Peak)

Figure 4 shows the current output across frequencies. The 5wt% sample produces the highest peak, generating approximately 0.011 A around 6 Hz. This peak, driven by resonance, enhances charge transfer within the material, increasing current output. The 7wt% sample peaks at around 0.008 A, while the 3wt% sample produces the lowest current output at around 0.006 A. The 5wt% concentration is optimal because it ensures efficient charge mobility without compromising the mechanical properties of the matrix. Excessive SnO₂ in the 7wt% sample increases rigidity, which may prevent the material from converting mechanical vibrations into electrical current efficiently. This finding suggests that further increases in SnO₂ content beyond 5wt% reduce current generation due to material stiffness [6].

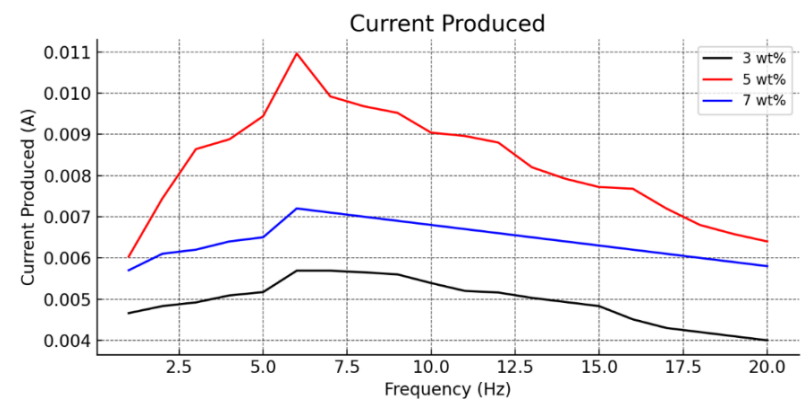


Fig. 4. Effect of different weight percent and frequency on Current Produced

Figure 5 shows power generation as a function of frequency. The 5wt% sample peaks at approximately 0.007 W around 6 Hz, a result of the combined peak voltage and current due to resonance. Since power is a function of both voltage and current, this resonance leads to maximum power output at the optimal frequency. The 7wt% sample generates a peak power of approximately 0.004 W, while the 3wt% sample shows the lowest power output at about 0.002 W. The 5wt% concentration provides the best balance between mechanical flexibility and charge mobility, leading to optimal power generation. At 7wt%, excessive filler content reduces flexibility and energy

conversion efficiency, resulting in lower power output. These results highlight that resonance at 6 Hz and the 5wt% SnO₂ content are ideal for maximizing power generation [22].

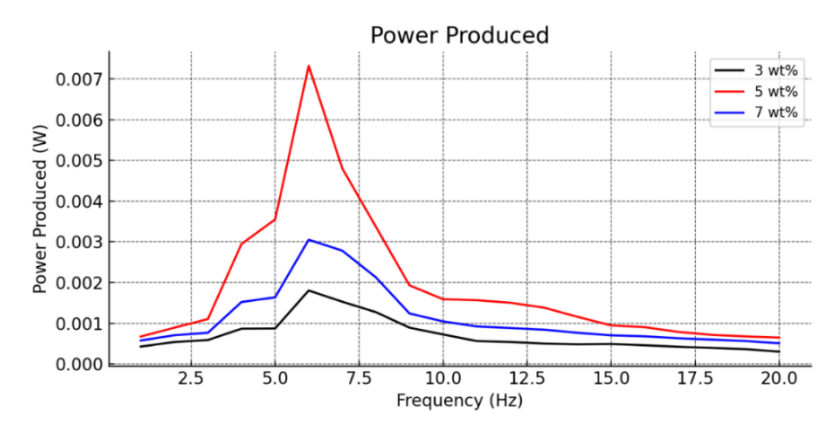


Fig. 5. Effect of different weight percent and frequency on Power

The resonance range of 5–7 Hz produced the highest voltage, current, and power outputs. This aligns with previous studies that also identified this frequency range as optimal for energy generation in similar nanocomposite systems, indicating a consistent correlation between frequency and efficiency enhancement [6,20]. The mechanistic insights suggesting that mechanical deformation at these specific frequencies enhances charge transfer efficiency and piezoelectric properties by amplifying the response of the nanocomposites.

Analysis of different SnO_2 concentrations revealed that 5 wt% is the most effective in maximizing piezoelectric performance. The composites at this concentration achieved a voltage output of 42V and a current density optimized for energy harvesting. This result is consistent with similar findings where the 5 wt% concentration was shown to balance charge mobility and the formation of the electroactive β -phase, which is critical for enhancing energy conversion efficiency [6,20]. These findings highlight the importance of maintaining this optimal concentration for achieving a balance between mechanical flexibility and energy efficiency.

Increasing SnO₂ concentration beyond the optimal level (7 wt%) negatively impacts performance. The results indicate that higher filler concentrations lead to increased stiffness, reducing the flexibility required for efficient charge generation. This is reflected in the observed decline in voltage outputs and power densities as stiffness impeded the material's capacity to respond to mechanical stress effectively [6]. Mechanistically, the rigidity introduced by excessive filler content limits the polymer matrix's deformation, which is crucial for piezoelectric charge generation. These findings align with other research that highlights the trade-offs between filler concentration and mechanical flexibility, emphasizing the need for balance to maintain optimal charge generation efficiency [20].

Composites with a low concentration of SnO₂ (3 wt%) showed consistent electrical outputs, particularly at lower frequencies. This stability is attributed to the enhanced flexibility of the polymer, which allows for better charge transfer. The minimal filler content (3 wt%) ensured steady voltage and current outputs, maintaining consistent performance under low-frequency mechanical stress [6]. However, while low concentrations stabilize performance, the power outputs remained lower compared to those at the optimal 5 wt% concentration, which achieved a maximum power density of up to 4900 W·m⁻³. At higher concentrations (7 wt%), increased stiffness led to reduced flexibility and, consequently, decreased performance due to the polymer's limited deformation capacity [19]. This demonstrates that maintaining flexibility in low-filler composites is essential for achieving effective charge transfer and efficient energy conversion.

3.2 Experimental Design Results

The x-axis of the graph represents the actual voltage (peak to peak) measured during the experiment, while the y-axis represents the predicted voltage calculated by the model. Figure 6 shows how well the model's predictions align with the actual experimental results. For example, when the actual voltage is 0.06 V, the predicted value is also close to 0.06 V, indicating accuracy. As the actual voltage increases to 0.175 V, the predicted value reaches 0.18 V, slightly overestimating the result. This comparison highlights the accuracy of the model across different voltage levels.

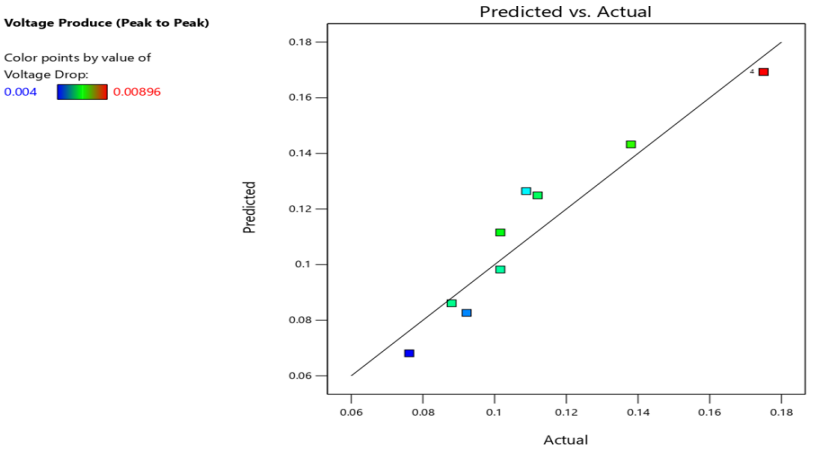


Fig. 6. Actual versus predicted results of Voltage Produced (Peak to Peak)

Figure 7 compares the predicted and actual power produced. The x-axis represents the actual power produced, while the y-axis shows the predicted power. The points are color-coded based on power values, ranging from 0.0003048 W (blue) to 0.001568 W (red). For example, an actual power of 0.0005 W has a corresponding predicted value of about 0.0005 W, indicating accuracy. However, for a higher actual power of 0.0015 W (red point), the predicted power is slightly higher, showing a small deviation. Overall, the model appears to provide reasonably accurate predictions.

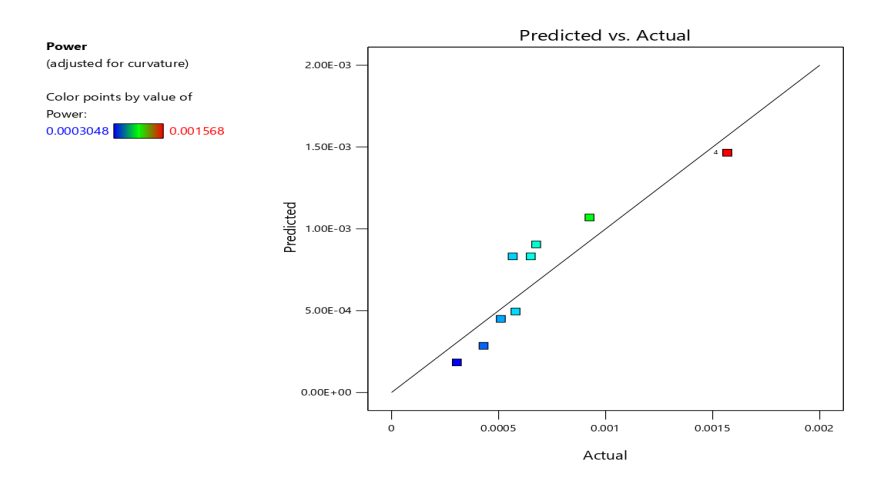


Fig. 7. Actual versus predicted results of Power

Figure 8 (a) contour plot shows the relationship between the weight percentage of SnO_2 (x-axis) and the frequency (y-axis) on the voltage produced (peak to peak). The voltage values are color-coded, ranging from 0.0762 V (blue) to 0.175 V (red). The red region in the center indicates that the

highest voltage, around 0.16 V, occurs at a weight percentage of 5 wt% and a frequency of around 10 Hz. The outer blue areas show lower voltages, particularly at lower weight percentages and frequencies. This plot helps visualize the optimal combination of factors for maximizing voltage.

Figure 8 (b) 3D surface plot shows the relationship between the weight percentage of SnO₂, frequency, and the voltage produced (peak to peak). The x-axis represents the weight percentage, the y-axis represents the frequency, and the z-axis shows the voltage produced. The color gradient indicates voltage values, ranging from 0.0762 V (blue) to 0.175 V (red). The highest voltage is observed around 5 wt% and a frequency of 10 Hz, with lower voltages occurring at lower frequencies and weight percentages. This visualization highlights optimal conditions for maximum voltage output.

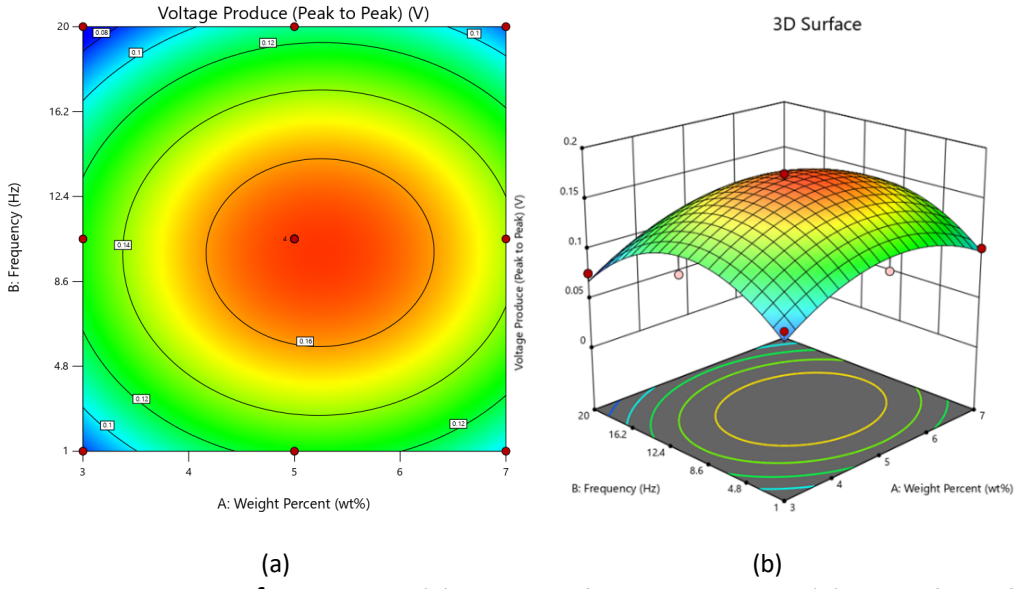


Fig. 8. Response surface method (a) Contour of voltage roduced; (b) 3D Surface of Voltage Produced

Figure 9 (a) contour plot shows the relationship between the weight percentage of SnO_2 (x-axis) and the frequency (y-axis) on the current produced. The current values are color-coded, ranging from 0.004 A (blue) to 0.00896 A (red). The red region in the center indicates the highest current of around 0.008 A occurs at a weight percentage of 5 wt% and a frequency of approximately 10 Hz. The outer blue and green areas represent lower currents, particularly at lower weight percentages and frequencies. This plot helps identify the optimal combination of factors for maximizing current output.

Figure 9 (b) 3D surface plot illustrates the relationship between the weight percentage of SnO₂ (x-axis), frequency (y-axis), and the current produced (z-axis). The current is color-coded, ranging from 0.004 A (blue) to 0.00896 A (red). The highest current is observed near 5 wt% SnO₂ and around 10 Hz frequency, represented by the red area on the surface. The outer areas, where the current is lower, are shown in blue and green. This visualization helps identify the optimal conditions for achieving maximum current output in the system.

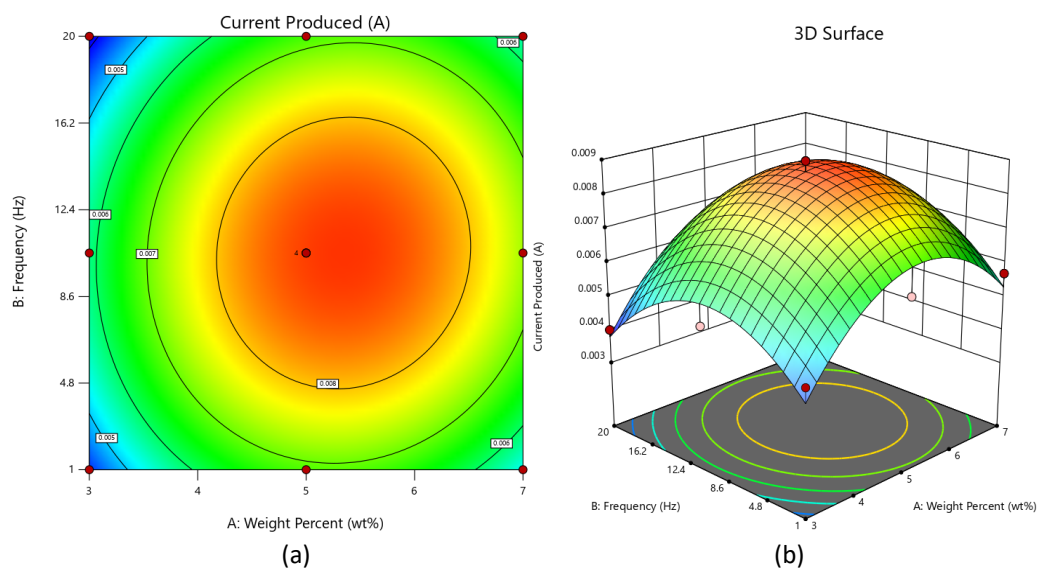


Fig. 9. Response Surface Method (a) Contour for Current Produced; (b) 3D Surface of Current Produced

Figure 10 (a) contour plot represents the relationship between the weight percentage of SnO_2 (x-axis), frequency (y-axis), and the power produced (W). The power values are color-coded, ranging from 0.0003048 W (blue) to 0.001568 W (red). The highest power output, around 0.0014 W, occurs at a weight percentage of 5 wt% and a frequency of approximately 10 Hz, as indicated by the red region in the center. The blue and green areas on the outer parts of the plot indicate lower power outputs, particularly at lower frequencies and weight percentages. This plot helps visualize the optimal combination of factors to maximize power generation.

Figure 10 (b) 3D surface plot illustrates the relationship between the weight percentage of SnO_2 (x-axis), frequency (y-axis), and the power produced (z-axis). The color gradient represents the power produced, ranging from 0.0003048 W (blue) to 0.001568 W (red). The highest power is generated at around 5 wt% SnO_2 and 10 Hz frequency, as shown by the peak in the red region. The outer areas of the plot, where the power output is lower, are represented by blue and green colors. This visualization provides insight into the optimal conditions for maximizing power generation from the system.

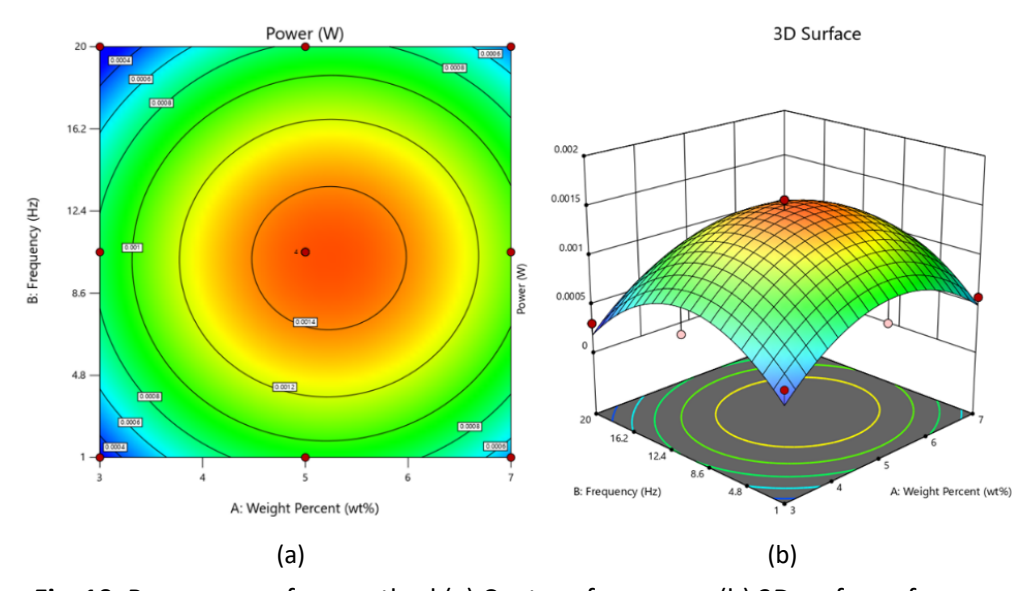


Fig. 10. Response surface method (a) Contour for power; (b) 3D surface of power

3.3 Numerical Optimization

In numerical optimization using Design-Expert 13, the software fits a model to the data and then sets goals for each factor and response. It uses these goals, such as maximizing or minimizing responses, to create a desirability function that combines the objectives into a single score. The software then searches for factor levels that maximize this score, identifying optimal conditions for the system. It provides visualizations like contour and 3D plots to show the effects of factors and validate the optimal solution. Simplification of non-significant factors may further improve the model's accuracy.

Table 4 outlines the criteria for numerical optimization in response surface methodology, specifying goals and limits for factors and responses. Weight Percent and Frequency are kept within ranges of 3 to 7 and 1 to 20, respectively. For responses, the objective is to maximize Voltage Produced (Peak to Peak) between 0.0762 and 0.175, minimize Voltage Drop within 0.004 to 0.00896, and maximize Current Produced from 0.004 to 0.00896. Additionally, Power is also set to be maximized, ranging between 0.0003048 and 0.001568. These criteria guide the optimization to achieve the most efficient conditions.

Table 4Criteria for numerical optimization

criteria for flamerical optimization			
Criteria	Goal	Lower Limit	Upper Limit
Weight Percent	In range	3	7
Frequency	In range	1	20
Voltage Produced (Peak to Peak)	Maximize	0.0762	0.175
Voltage Drop	Minimize	0.004	0.00896
Current Produced	Maximize	0.004	0.00896
Power	Maximize	0.0003048	0.001568

Table 5 shows the optimization results of two viable solutions, with Solution 1 selected due to its higher desirability score of 0.584. Both solutions meet the set criteria for weight percent, frequency, voltage, current, and power, staying within the defined ranges. Solution 1 produces a higher voltage (0.154) and maintains the desired current (0.008), making it the better choice. The overall desirability score suggests that the optimization is moderately successful, but there is room for improvement. While the results are acceptable, further refinement could increase the desirability score and optimize performance further.

Table 5Solution design optimization

Number	Weight Percent	Frequency	Voltage Produce (Peak to Peak)	Voltage Drop	Current Produced	Power	Desirability	
1	3.870	9.756	0.154	0.008	0.008	0.001	0.584	Selected
2	6.643	8.316	0.152	0.008	0.008	0.001	0.563	

4. Conclusion

All PVDF/SnO $_2$ FPENG films exhibited hydrophobic behavior, supporting their durability in device applications. The electrical output of the composites was evaluated across a frequency range of 1 $^-$ 20 Hz for 3 wt%, 5 wt%, and 7 wt% SnO $_2$ loadings. The 5 wt% sample consistently outperformed the others, generating peak voltage values above 0.6 V and delivering the highest current and power

output at approximately 6 Hz. These results indicate that 5 wt% SnO₂ offers an optimal balance between filler content and energy conversion efficiency.

Electrical output increased notably between 5 Hz and 7 Hz for all samples, identifying this range as the most effective for energy harvesting. However, performance declined beyond 7 Hz, particularly for the 7 wt% sample, which showed signs of diminishing returns due to possible filler agglomeration. The 3 wt% sample, while less efficient overall, maintained stable performance at lower frequencies. These findings highlight the need to tailor SnO₂ concentration to specific operating conditions. For applications harvesting energy from low- to mid-frequency vibrations, a 5 wt% SnO₂ concentration provides the most effective trade-off between material performance and functional reliability.

Acknowledgement

This research was not funded by any grant.

References

- [1] AlAhzm, Abdulrahman Mohmmed, Maan Omar Alejli, Deepalekshmi Ponnamma, Yara Elgawady, and Mariam Al Ali Al-Maadeed. "Piezoelectric properties of zinc oxide/iron oxide filled polyvinylidene fluoride nanocomposite fibers." *Journal of Materials Science: Materials in Electronics* 32, no. 11 (2021): 14610-14622. https://doi.org/10.1007/s10854-021-06020-3
- [2] Das, Tupan, Sushree Nibedita Rout, Amar Dev, and Manoranjan Kar. "The MnAl-alloy nanoparticles incorporated PVDF-based piezoelectric nanogenerator as a self-powered real-time pedometer sensor." *Applied Physics Letters* 125, no. 16 (2024). https://doi.org/10.1063/5.0219148
- [3] Gupta, Namrata, Abhishek Ray, Alok Naugarhiya, and Abhinav Gupta. "Design and optimization of MEMS piezoelectric cantilever for vibration energy harvesting application." In *Advances in VLSI, Communication, and Signal Processing: Select Proceedings of VCAS 2018*, pp. 655-662. Singapore: Springer Singapore, 2019. https://doi.org/10.1007/978-981-32-9775-3 60
- [4] Hasanzadeh, Mahdi, Mohammad Reza Ghahhari, and Seyed Mansour Bidoki. "Enhanced piezoelectric performance of PVDF-based electrospun nanofibers by utilizing in situ synthesized graphene-ZnO nanocomposites." *Journal of Materials Science: Materials in Electronics* 32, no. 12 (2021): 15789-15800. https://doi.org/10.1007/s10854-021-06132-w
- [5] He, Xianming, Quan Wen, Zhiyu Wen, and Xiaojing Mu. "A MEMS piezoelectric vibration energy harvester based on trapezoidal cantilever beam array." In 2020 IEEE 33rd International Conference on Micro Electro Mechanical Systems (MEMS), pp. 532-535. IEEE, 2020. https://doi.org/10.1109/MEMS46641.2020.9056434
- [6] Kar, Epsita, Navonil Bose, Biplab Dutta, Sudarshana Banerjee, Nillohit Mukherjee, and Sampad Mukherjee. "2D SnO2 nanosheet/PVDF composite based flexible, self-cleaning piezoelectric energy harvester." Energy conversion and management 184 (2019): 600-608. https://doi.org/10.1016/j.enconman.2019.01.073
- [7] Kim, Moonkeun, Sang-Kyun Lee, Yil Suk Yang, Jaehwa Jeong, Nam Ki Min, and Kwang-Ho Kwon. "Design and fabrication of vibration based energy harvester using microelectromechanical system piezoelectric cantilever for low power applications." *Journal of nanoscience and nanotechnology* 13, no. 12 (2013): 7932-7937. https://doi.org/10.1166/jnn.2013.8106
- [8] Manikandan, M., P. Rajagopalan, Nandini Patra, S. Jayachandran, M. Muralidharan, SS Mani Prabu, I. A. Palani, and Vipul Singh. "Development of Sn-doped ZnO based ecofriendly piezoelectric nanogenerator for energy harvesting application." *Nanotechnology* 31, no. 18 (2020): 185401. https://doi.org/10.1088/1361-6528/ab6b9e
- [9] Masara, David Omooria, Hassan El Gamal, and Ossama Mokhiamar. "Split cantilever multi-resonant piezoelectric energy harvester for low-frequency application." *Energies* 14, no. 16 (2021): 5077. https://doi.org/10.3390/en14165077
- [10] Chakhchaoui, Nabil, Rida Farhan, Adil Eddiai, Mounir Meddad, Omar Cherkaoui, M'hamed Mazroui, Yahia Boughaleb, and Lieva Van Langenhove. "Improvement of the electroactive β-phase nucleation and piezoelectric properties of PVDF-HFP thin films influenced by TiO2 nanoparticles." *Materials today: proceedings* 39 (2021): 1148-1152. https://doi.org/10.1016/j.matpr.2020.05.407
- [11] Oliva, Francisco Sebastian Navarro, Sanjeeva N. Murthy, Luc Lenglet, Alejandro Ospina, Steven Weigand, and Fahmi Bedoui. "In-situ WAXS and SAXS microstructural investigation of Poly (vinylidene fluoride)-Fe3O4 coaxial-electrospun nanocomposites under thermal and mechanical loading: Nanoparticles size effects on fibers molecular orientation, mechanical properties and crystalline polymorphs." *Polymer* 308 (2024): 127406. https://doi.org/10.1016/j.polymer.2024.127406

- [12] Ojha, Devi Prashad, Bhavana Joshi, Edmund Samuel, Ashwin Khadka, Ali Aldalbahi, Govindasami Periyasami, Daekyu Choi, Seongpil An, and Sam S. Yoon. "Supersonically sprayed flexible ZnO/PVDF composite films with enhanced piezoelectricity for energy harvesting and storage." *International Journal of Energy Research* 2023, no. 1 (2023): 3074782. https://doi.org/10.1155/2023/3074782
- [13] de Oliveira, Felipe A. Costa, Davies William de Lima Monteiro, and Dalton Martini Colombo. "Design, modeling, characterization and analysis of a low frequency micro-fabricated piezoelectric cantilever for vibration sensing and energy harvesting applications." Sensors and Actuators A: Physical 326 (2021): 112709. https://doi.org/10.1016/j.sna.2021.112709
- [14] Rahimzadeh, Mohammad, Hamid Samadi, and Nikta Shams Mohammadi. "Analysis of energy harvesting enhancement in piezoelectric unimorph cantilevers." *Sensors* 21, no. 24 (2021): 8463. https://doi.org/10.3390/s21248463
- [15] Rasoolzadeh, Mina, Zahra Sherafat, Mehran Vahedi, and Elham Bagherzadeh. "Structure dependent piezoelectricity in electrospun PVDF-SiC nanoenergy harvesters." *Journal of Alloys and Compounds* 917 (2022): 165505. https://doi.org/10.1016/j.jallcom.2022.165505
- [16] Sadikbasha, Shaik, B. Radhika, and V. Pandurangan. "Auxetic hexachiral cantilever beams for piezoelectric vibration energy harvesting." *Smart Materials and Structures* 31, no. 10 (2022): 105015. https://doi.org/10.1088/1361-665X/ac8d3e
- [17] Saikh, Md Minarul, Nur Amin Hoque, Prosenjit Biswas, Wahida Rahman, Namrata Das, Sukhen Das, and Pradip Thakur. "Self-Polarized ZrO2/Poly (vinylidene fluoride-co-hexafluoropropylene) nanocomposite-based piezoelectric nanogenerator and single-electrode triboelectric nanogenerator for sustainable energy harvesting from human movements." *physica status solidi (a)* 218, no. 9 (2021): 2000695. https://doi.org/10.1002/pssa.202000695
- [18] Sang, Yingjun, Yuanyuan Fan, Fangxiu Wang, Xiaoxin Zhang, Yan Yang, and Ming Zhang. "Vibration detection technology research based on piezoelectric cantilever." *Mechanics of Advanced Materials and Structures* 29, no. 24 (2022): 3588-3594. https://doi.org/10.1080/15376494.2022.2075060
- [19] Sasmal, Abhishek, Samar Kumar Medda, P. Sujatha Devi, and Shrabanee Sen. "Nano-ZnO decorated ZnSnO 3 as efficient fillers in PVDF matrixes: Toward simultaneous enhancement of energy storage density and efficiency and improved energy harvesting activity." *Nanoscale* 12, no. 40 (2020): 20908-20921. https://doi.org/10.1039/D0NR02057E
- [20] Karan, Sumanta Kumar, Dipankar Mandal, and Bhanu Bhusan Khatua. "Self-powered flexible Fe-doped RGO/PVDF nanocomposite: an excellent material for a piezoelectric energy harvester." *Nanoscale* 7, no. 24 (2015): 10655-10666. https://doi.org/10.1039/C5NR02067K
- [21] Song, Jundong, Guanxing Zhao, Bo Li, and Jin Wang. "Design optimization of PVDF-based piezoelectric energy harvesters." *Heliyon* 3, no. 9 (2017). https://doi.org/10.1016/j.heliyon.2017.e00377
- [22] Subudhi, Poonam, Vikas Sagar, Santosh Kumar, and Deepak Punetha. "Simulation and optimization of substrate layer material for PVDF cantilever based vibration energy harvesting system." *IEEE Sensors Journal* 23, no. 23 (2023): 28689-28695. https://doi.org/10.1109/JSEN.2023.3326681
- [23] Tuma, Chuttipong, and Danai Phaoharuhansa. "Vibration Energy Harvest for Low Frequency using Double-piezoelectric Cantilever Beam." In *MATEC Web of Conferences*, vol. 306, p. 04006. EDP Sciences, 2020. https://doi.org/10.1051/matecconf/202030604006
- [24] Uddin, Md Naim, Md Shabiul Islam, M. Faisal Riyad, and M. S. Bhuyan. "Finite element analysis of piezoelectric cantilever beam using vibration for energy harvesting devices." In *AIP Conference Proceedings*, vol. 2324, no. 1, p. 030004. AIP Publishing LLC, 2021. https://doi.org/10.1063/5.0037801
- [25] Yang, Jie, Yihe Zhang, Yanan Li, Zhihao Wang, Wenjiang Wang, Qi An, and Wangshu Tong. "Piezoelectric nanogenerators based on graphene oxide/PVDF electrospun nanofiber with enhanced performances by in-situ reduction." *Materials Today Communications* 26 (2021): 101629. https://doi.org/10.1016/j.mtcomm.2020.101629
- [26] Liu, Jing-Quan, Hua-Bin Fang, Zheng-Yi Xu, Xin-Hui Mao, Xiu-Cheng Shen, Di Chen, Hang Liao, and Bing-Chu Cai. 2008. "A MEMS-Based Piezoelectric Power Generator Array for Vibration Energy Harvesting." *Microelectronics Journal* 39 (5): 802–6. https://doi.org/10.1016/j.mejo.2007.12.017
- [27] Zhao, Qiuying, Lu Yang, Kaineng Chen, Yizhou Ma, Qirui Peng, Hongli Ji, and Jinhao Qiu. "Flexible textured MnO2 nanorods/PVDF hybrid films with superior piezoelectric performance for energy harvesting application." *Composites Science and Technology* 199 (2020): 108330. https://doi.org/10.1016/j.compscitech.2020.108330
- [28] Singh, Huidrom Hemojit, Simrjit Singh, and Neeraj Khare. "Enhanced β-phase in PVDF polymer nanocomposite and its application for nanogenerator." *Polymers for Advanced Technologies* 29, no. 1 (2018): 143-150. https://doi.org/10.1002/pat.4096
- [29] Ting, Yung, Suprapto, Naveen Bunekar, Kulandaivel Sivasankar, and Yopan Rahmad Aldori. "Using annealing

treatment on fabrication ionic liquid-based PVDF films." *Coatings* 10, no. 1 (2020): 44. https://doi.org/10.3390/coatings10010044